Title

DNA METABOLISM AND DEVELOPMENT OF ORGANELLES IN GUINEA-PIG MEGAKARYOCYTES: A COMBINED ULTRASTRUCTURAL AUTORADIOGRAPHIC AND CYTOPHOTOMETRIC STUDY

Author

Paulus, Jean-Michel.

Publication Date

1969-05-01

Submitted in part to Blood

UCRL-19201
Preprint

DNA METABOLISM AND DEVELOPMENT OF ORGANELLES IN GUINEA-PIG MEGAKARYOCYTES: A COMBINED ULTRASTRUCTURAL, AUTORADIOGRAPHIC AND CYTOPHOTOMETRIC STUDY

Jean-Michel Paulus

May 1969

AEC Contract No. W-7405-eng-48

LAWRENCE RADIATION LABORATORY
UNIVERSITY of CALIFORNIA BERKELEY

UCRL-19201

DISCLAIMER

DNA METABOLISM AND DEVELOPMENT OF ORGANELLES IN GUINEA-PIG MEGAKARYOCYTES: A COMBINED ULTRASTRUCTURAL, AUTORADIOGRAPHIC AND CYTOPHOTOMETRIC STUDY

By Jean-Michel Paulus

Numerous analyses have been made of the relationships between cell differentiation and proliferation (1-6). Light microscopy studies show that megakaryocytes specialize in two steps: first, a series of DNA syntheses leads to the final ploidy level of 8N, 16N, 32N or 64N (7-16); secondly, cytoplasm matures by losing its basophilia, acquiring granules (10, 15) and platelet antigens (15) and finally liberating platelets (17). In the present study, the alternate thick and thin section technique was used to explore the relationship between "ploidization" and cytoplasmic maturation on the ultrastructural level. It was found that the synthesis of specific organelles began during the ploidization phase and increased considerably when this process had stopped after an average of 3 DNA syntheses.

From the Institut de Pathologie Cellulaire, Hopital de Bicêtre, 94-Le Kremlin-Bicêtre, France (Prof. M. Bessis), and the Donner Laboratory, University of California, Berkeley (Prof. H. C. Mel).

Presented at the Meeting of the Société Française d'Hématologie, December 18, 1967 and at the Meeting of the Federation of Associated Societies of Experimental Biology, Atlantic City, April 18, 1969.

Supported by a grant from the French Government.

JEAN-MICHEL PAULUS M.D.: Chargé de Recherches au Fonds Belge de la Recherche Scientifique. Present Address: Institut de Médecine, Departement de Clinique et Pathologie Médicales (Prof. H. Van Cauwenberge, Assoc. Prof. J. Hugues), University of Liège, Belgium.

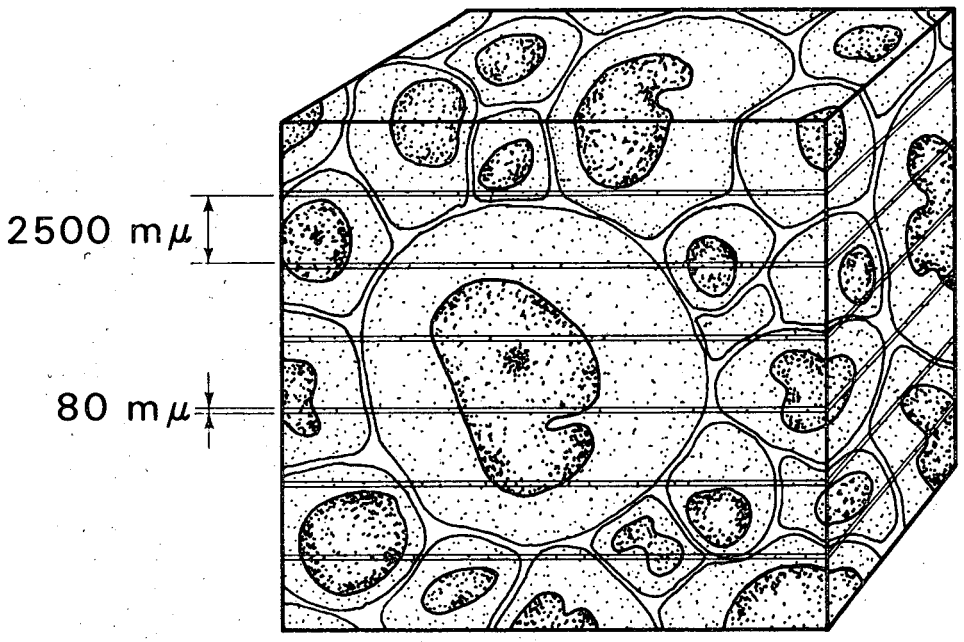

DBL 694-4624

Fig 1. Scheme of marrow sectioning, showing megakaryocyte cut into 5 thick and 4 thin sections. For clarity, thin sections were magnified out of proportion to thick sections about three times.

MATERIAL AND METHODS

Preparation of sections

Guinea-pigs weighing 300 gr were used. Small blocks of bone marrow were fixed in 1% osmium tetroxide for 7 min. Short fixation times in osmium have been shown to be adequate in many materials (18). These were preferred in the present study to try to minimize the non specific loss of transmission (NSLT) associated with this fixative. Glutaraldehyde was avoided because of its reaction with the Schiff reagent which introduces a diffuse staining of bone marrow cells. After fixation, the blocks of marrow were dehydrated and embedded in epon. They were then cut into series of alternate thick (about 2.5μ) and thin (about 0.08μ) sections with an LKB ultramicrotome (figs 1 and 2), care being taken to minimize the loss of material so that the megakaryocytes might be studied in totality. This cutting thus divided each megakaryocyte into 4 to 10 pairs of sections, depending on the size of the cell.

Microspectrophotometric measurements of DNA

The thick sections of osmium-fixed material, containing about 96% of the megakaryocyte nuclei, were dehydrated and stained by the Feulgen method (19). Non specific staining by the Schiff reagent was absent or negligible. However, osmium fixation introduced a non specific loss of transmission (NSLT) both in the nucleus and the cytoplasm. Although this NSLT in the past did not prevent Feulgen measurements of DNA (20), it invalidated uncorrected scanning measurements, which cannot be limited strictly to the nucleus. The NSLT, highest at 400mμ, (fig 3) is explained by the light scattering caused by osmium-fixed subcellular particles (21). The extinction spectrum over the nucleus was approximately the sum of the NSLT and the extinction of formol-fixed nuclei stained by the Feulgen

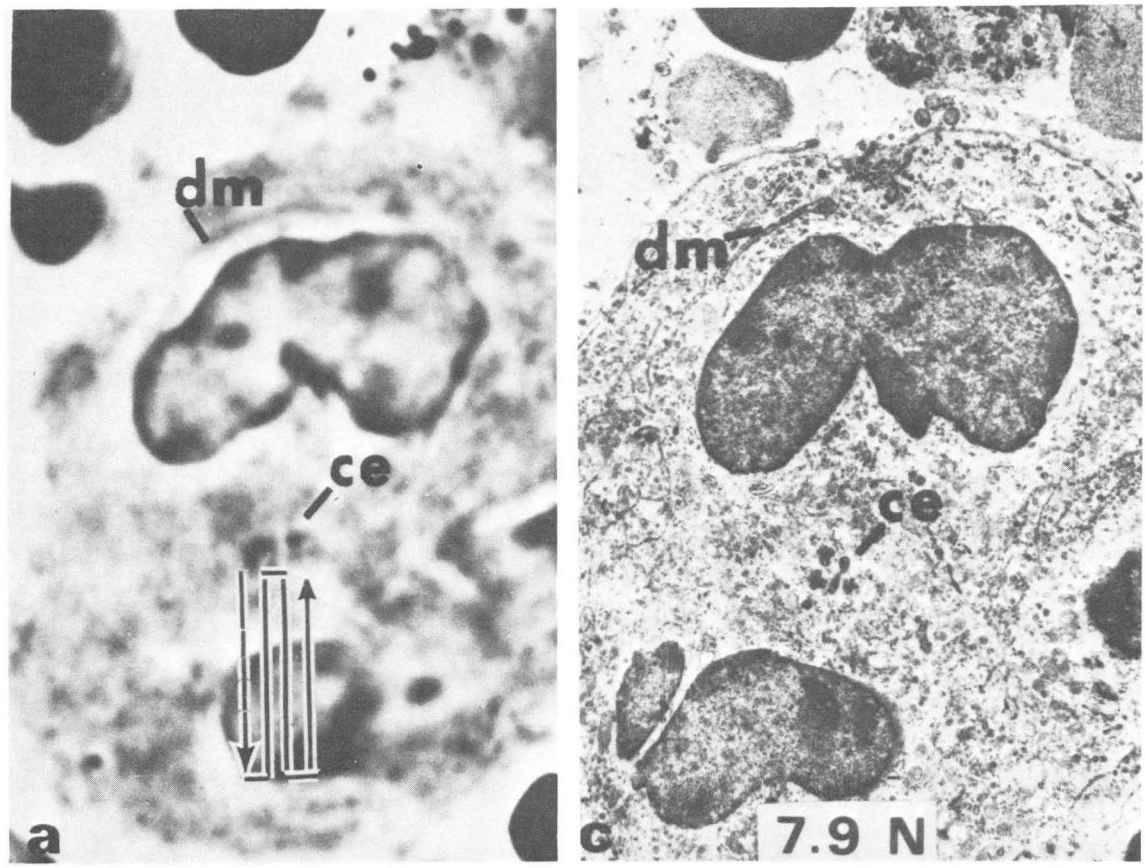

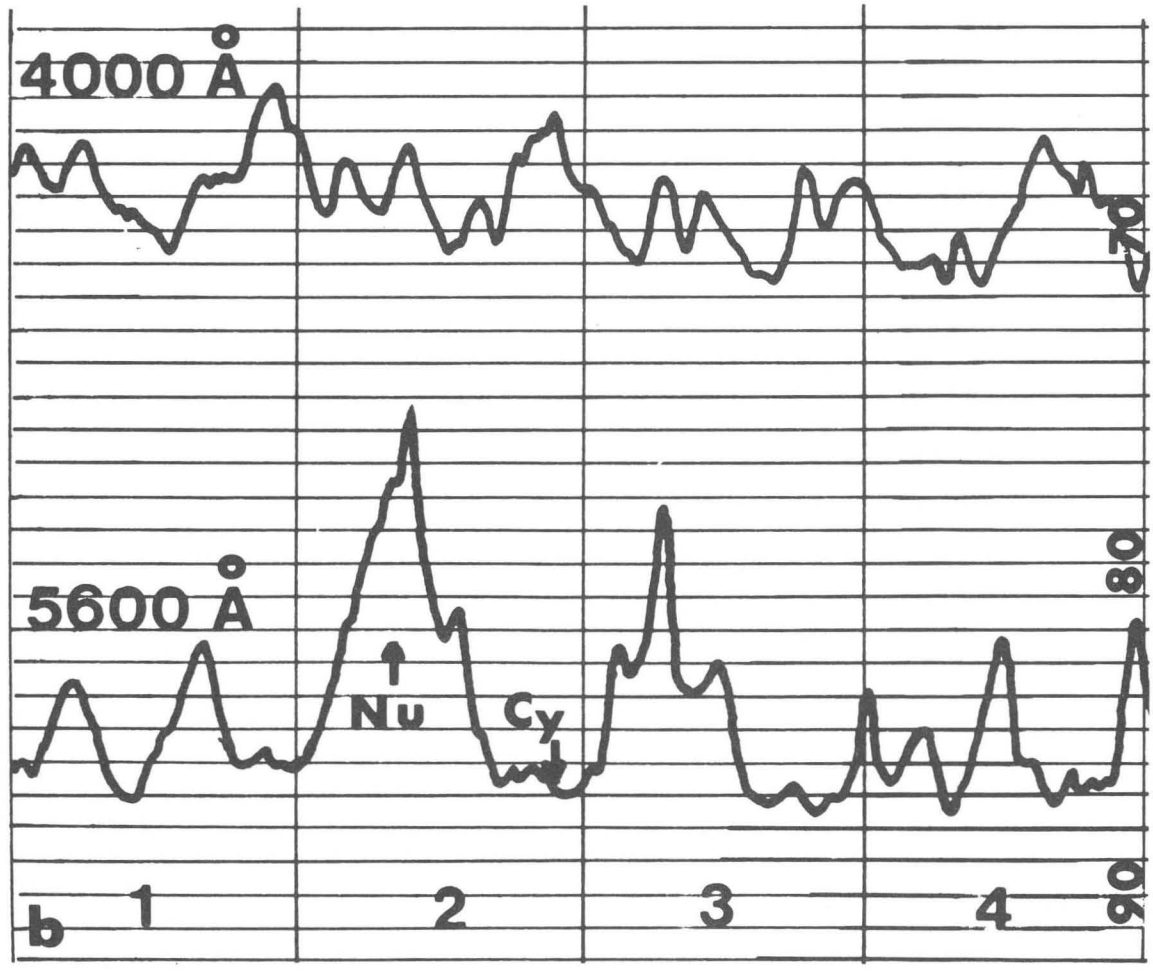

XBB 695-3218

Symbols of abbreviations: ch chromosome. ce centriole. cy cytoplasm. dm demarcation membrane. g Gogli apparatus. gr granule. m mitochondria. N ploidy value. nc nucleolus. nu nucleus. pl platelet. rer rough endoplasmic reticulum. v vessel.

Fig 2. Illustration of method. Fig 2a. Phase contrast micrograph of 3 μ section of osmium-fixed megakaryocyte, stained by Feulgen method. Centrioles (ce) and one demarcation membrane (dm) are conspicuous. X 6375. Fig 2b. Portion of recording of DNA measurement made on above megakaryocyte. The section of nucleus was scanned along the four adjacent lines (numbered 1 to 4), each 1 μ wide and the light transmission was recorded at both 5600 Å and 4000 Å. The measurement at 4000 Å permits correction for the 13% nonspecific loss of transmission created by osmium fixation and allows calculation of the ploidy value, 7.9N (see methods). Fig 2c. Electron micrograph of thin section contiguous to thick section in Fig 2a., showing maturing megakaryocyte with demarcation membranes (dm), granules, 4 centrioles (ce), ribosomes and rough endoplasmic reticulum. X6375.

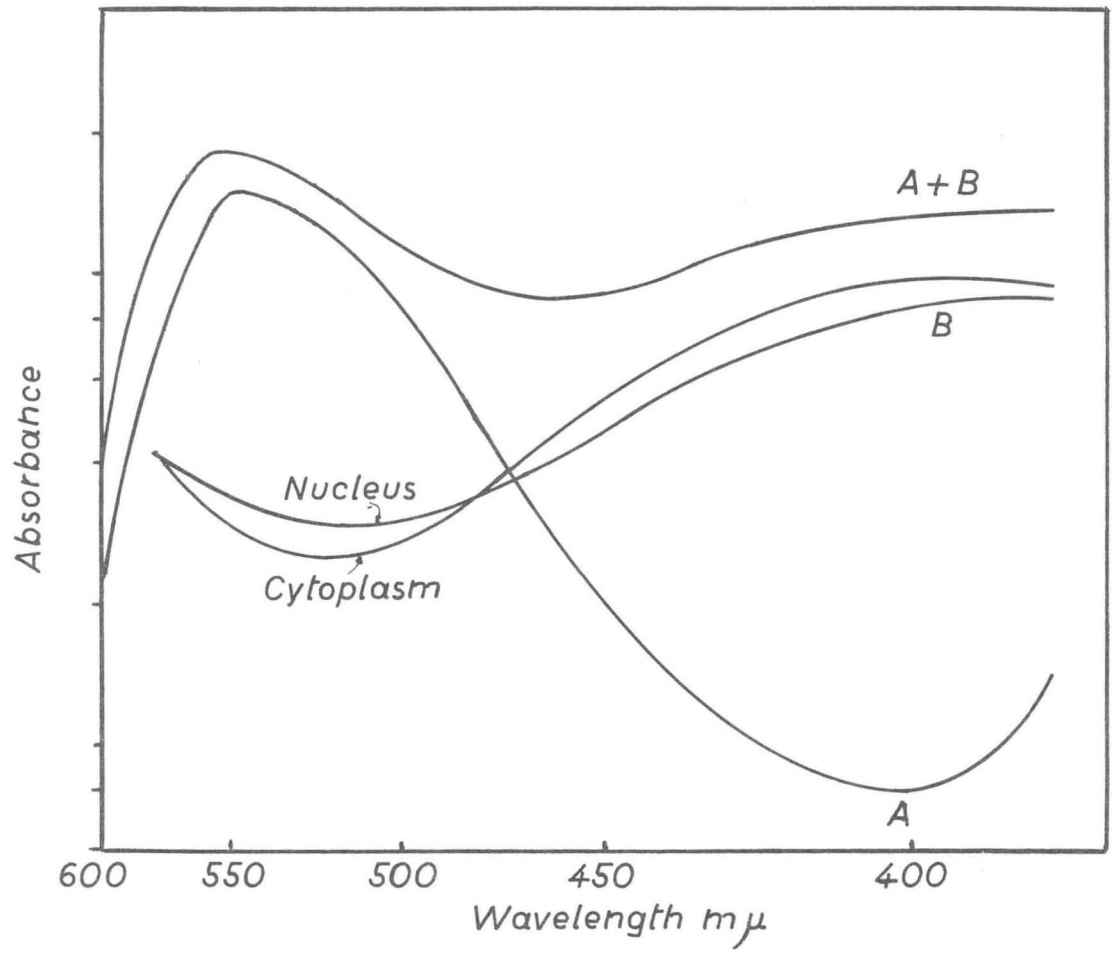

XBL 692-261

Fig 3. Extinction curves of megakaryocytes. A: nucleus in bone marrow smear fixed with formol and stained by Feulgen method. B: nucleus (nu) and cytoplasm (cy) in a section of marrow following osmium fixation, epon embedding and Feulgen procedure, omitting staining by Schiff reagent. C: nucleus in a section of marrow following osmium fixation, epon embedding and complete Feulgen procedure. Cytoplasmic curve was similar to B or showed a small, negligible peak at 560 mμ. Curves were plotted as logarithm extinction, using arbitrary units so that their shape might be made independent of concentration of absorbing material (22).

method (fig. 3). In addition, the Feulgen extinction on the latter material at 400mμ was only about 7% of that measured at 560 mμ. Since the spectrum of the NSLT was almost the same in both cytoplasm and nucleus (fig 3), the Feulgen negative cytoplasm served as a "baseline" NSLT control for each nucleus measured. Consequently, the specific Feulgen extinction at 560 mμ could be calculated according to the following formula

$$F_{560} = E_{560} - \frac{E_{400}}{k}$$

in which E_{560} and E_{400} represent the measured extinction at 560 and 400 mμ respectively and k (which varied between 2 and 4) is the ratio of $NSLT_{400}$ to $NSLT_{560}$ measured in the absorbing cytoplasm (see fig. 2). Scanning microspectrophotometry was performed with the Zeiss UMSP1 operated with an ultrafluar objective 100 X, NA 1.25 and a condenser NA 0.3. The scanning interval and the diameter of the measuring diaphragm were 1 μ (†). The total DNA of each megakaryocyte was calculated by adding up the amounts measured for each section, and the ploidy value was determined from similar measurements made on orthochromatic normoblasts, known to be diploid (23).

Autoradiographic studies

Labeling of DNA-synthesizing megakaryocytes was carried out in vitro as described by Rubini et al (24). Blocks of guinea-pig marrow were incubated for 1 hour at 37° C in a labeling solution consisting of 1 ml of fetal calf serum and 20 μCi of thymidine methyl ^3H, specific activity 15C/mM (CEN, Mol, Belgium). After washing with fetal calf serum, the blocks were then fixed with a 6% glutaraldehyde solution in phosphate buffer at p.H 7.0, post-fixed for 40 min. in 1% osmium tetroxide in phosphate buffer and finally

(†) In preliminary experiments conducted by the multiple plug method, no significant difference in mean nuclear extinction was found when diaphragms of 0.32 μ or 1 μ were used.

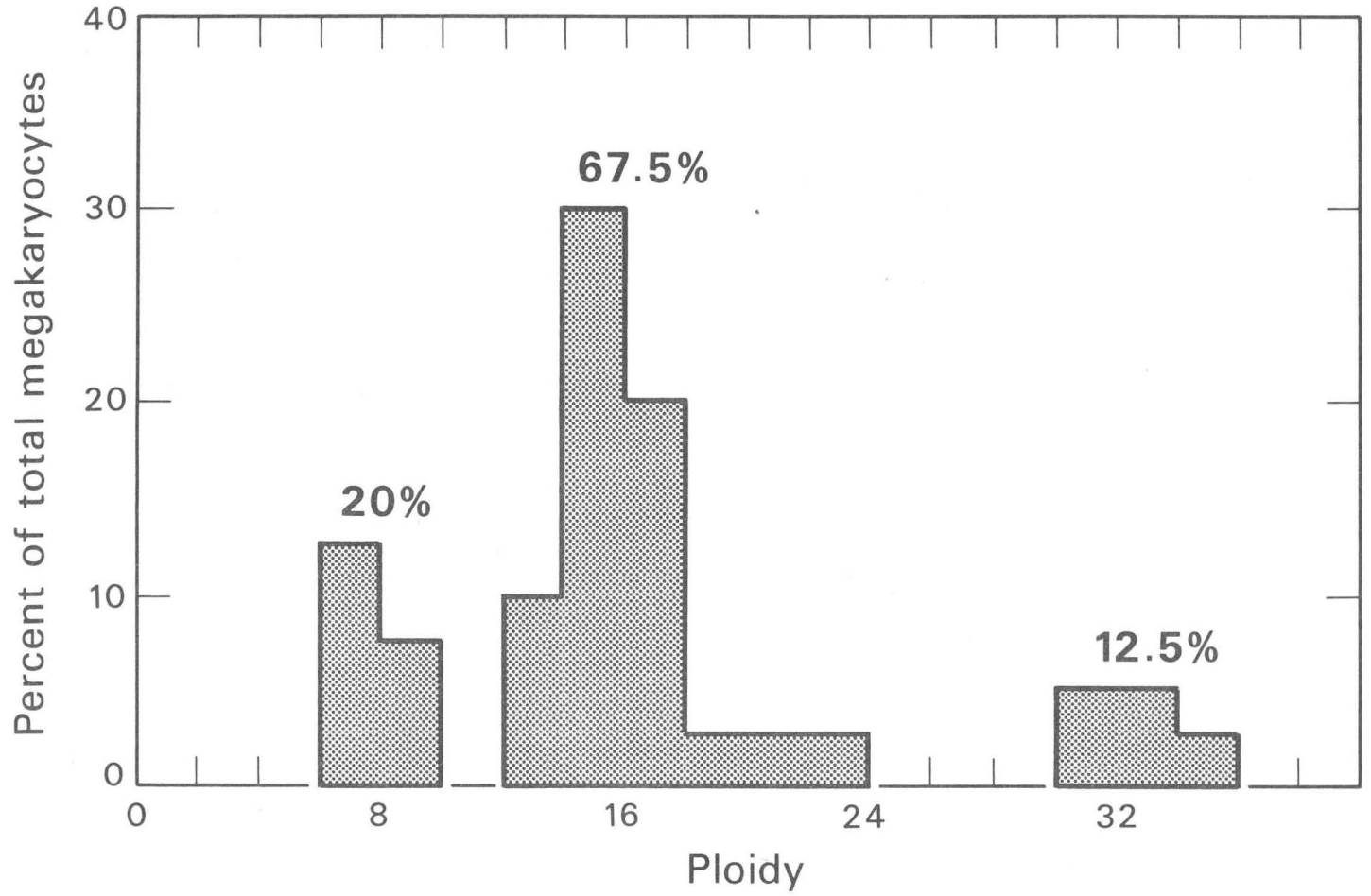

DBL 692-4555

Fig 4. Histogram of ploidy values of guinea-pig megakaryocytes, using the above described technique.

embedded in epon.

Alternate thick and thin sections were cut, as described above. The thick sections were placed on a glass slide, covered with Kodak AR 10 stripping film and exposed for 5 weeks. Subsequently, the slides were developed for 6 min. in Kodak D170 developer and fixed for 6 min. in thiosulfate fixer. Finally, they were mounted and examined in phase contrast microscopy.

Electron Microscopy

The thin sections were stained by uranyl acetate and lead citrate (25) and examined under a Siemens or a Hitachi electron microscope, operated at 80 or 75 KV, to assess the stage of the cell cytoplasmic maturation. Low magnification photographs of the thick sections were used to correlate the microspectrophotometric or autoradiographic findings on each megakaryocyte with its electron microscopic characteristics (figs 2, 5 and 7).

RESULTS

Relationship between DNA synthesizing ability and cytoplasmic maturation

(1) Ultrastructure of megakaryocytes during the ploidization phase

"Immature megakaryocytes" (†) were studied by analysis of both DNA synthesizing and mitotic cells. Megakaryocytes incorporating thymidine had, in addition to the high nuclear-cytoplasmic ratio, two distinctive character-

---

(†) Immature megakaryocytes corresponded to megakaryoblasts in Bessis' nomenclature (26) and not to basophile megakaryocytes (27), which are non DNA synthesizing cells (15). The term immature was used here since it was felt that the name megakaryoblast should be reserved to cells younger than those described in this study. Maturing megakaryocytes corresponded to Bessis' basophile and granular megakaryocytes.

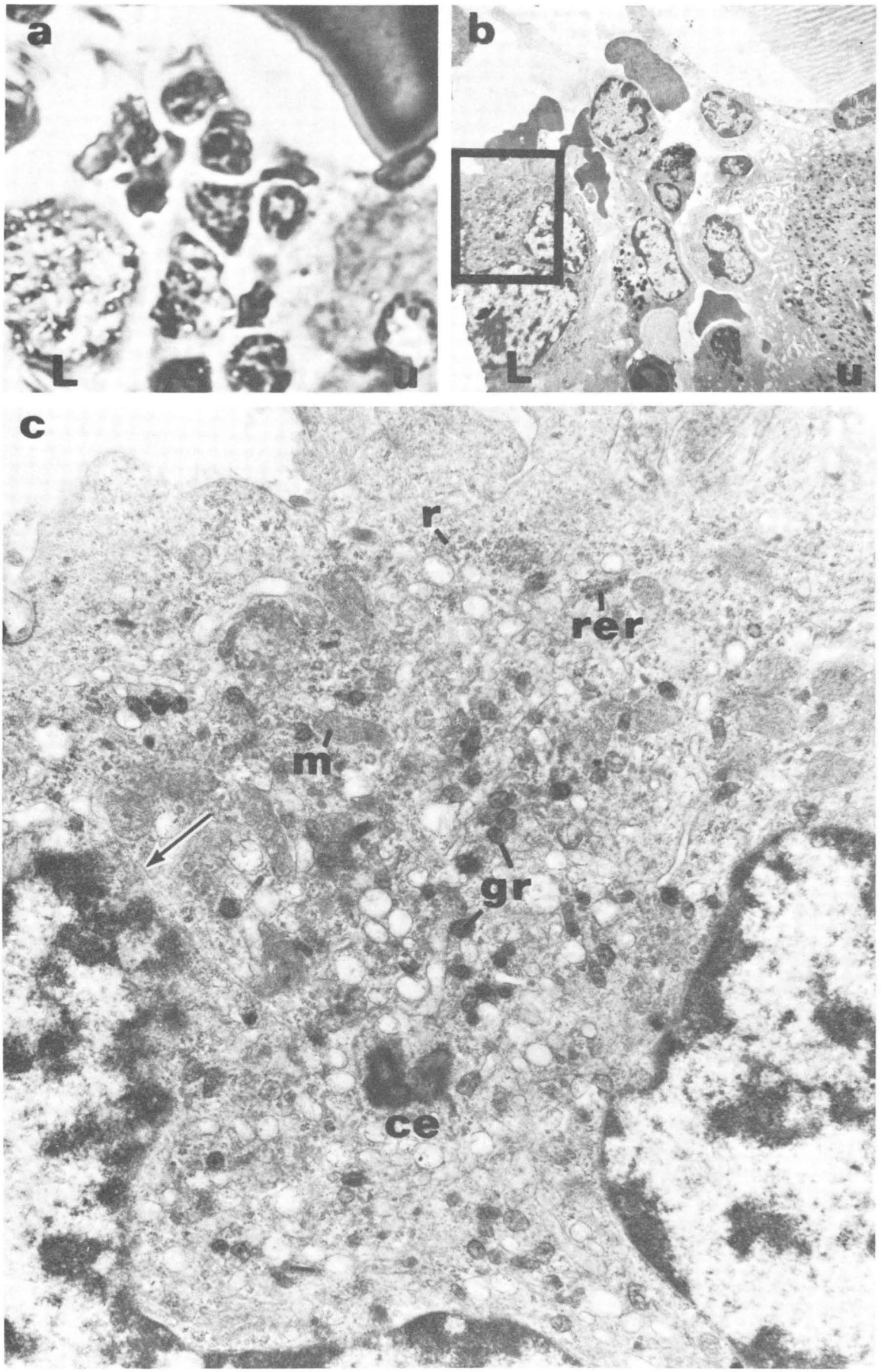
a
L
u
b
L
u
c
r
rer
m
gr
ce

XBB 695-3215

Fig 6. Sections through "immature" megakaryocytes. a and b: showing hollow nucleus. Autoradiography of adjacent thick section demonstrated thymidine incorporation. Glutaraldehyde and osmium fixation X approximately 3500. c: Section through top of nucleus. Ring shaped nucleus is visible on next sections. Ploidy value is indicated. Osmium fixation X 7300.

Fig 5. "Immature" megakaryocyte synthesizing DNA. 5a: Autoradiogram of thick section of marrow incubated for 1 hour in ^{3}H thymidine showing unlabeled (u) and labeled (L) megakaryocytes. Basic fuchsin staining, phase contrast X1950. 5b: Thin section corresponding to 5a. 5c: Endonuclear zone of same cell showing granule formation in Golgi zone. Arrow points to microtubule presumably attached to centriole ce. Glutaraldehyde osmium fixation X 13600.

istics. 1) In the majority of sections, the center of the nucleus was hollow suggesting that the nucleus assumes roughly the shape of a hollow-centered sphere (figs 5 and 6). In sections cut through the top of the nucleus (fig 6c) and possibly also in the youngest cells (fig 7), the endonuclear zone was reduced to thin cytoplasmic extensions communicating with the rest of the cytoplasm. 2) Although immaturity was evident from the abundance of ribosomes and polyribosomes, well developed nucleoli, and the rather diffuse nuclear pattern (figs 5, 6 and 7), a small number of the specific organelles were already formed in the youngest recognizable megakaryocytes. The endonuclear zone contained a large Golgi apparatus, often extending into the exonuclear cytoplasm (figs 5 and 6), and known to be synthesizing the early granules (fig 5; ref. 28). Microtubules were seen attached to the centrioles (fig 5) or at the periphery of the cytoplasm (fig 10), while in other pictures, they were accompanied by myofibrils. Demarcation membranes were also found in immature cells. In addition to these organelles, immature megakaryocytes contained many mitochondria and profiles of rough endoplasmic reticulum (fig 5). 17.5% of megakaryocytes had the cytological characteristics described above.

In mitotic megakaryocytes, granules(fig 8 and 9), demarcation membranes (fig 9) and microtubules (fig 10) were similarly visible.

(2) Ultrastructure of megakaryocytes after the ploidization phase

Maturing megakaryocytes represented the majority (67.5%) of the recognizable elements of the series. Although in some sections, hollow nuclei were still visible, their frequency diminished with maturation. Cytoplasmic development in these cells involves, in addition to extensive granule synthesis, formation of large amounts of demarcation membranes (29), (figs 12 and 13) which eventually delineate the future platelet territories (fig 13c). Since the formation of membranes is restricted to the intermediate part of the cytoplasm, the latter becomes divided into three concentric zones. The inner zone has an

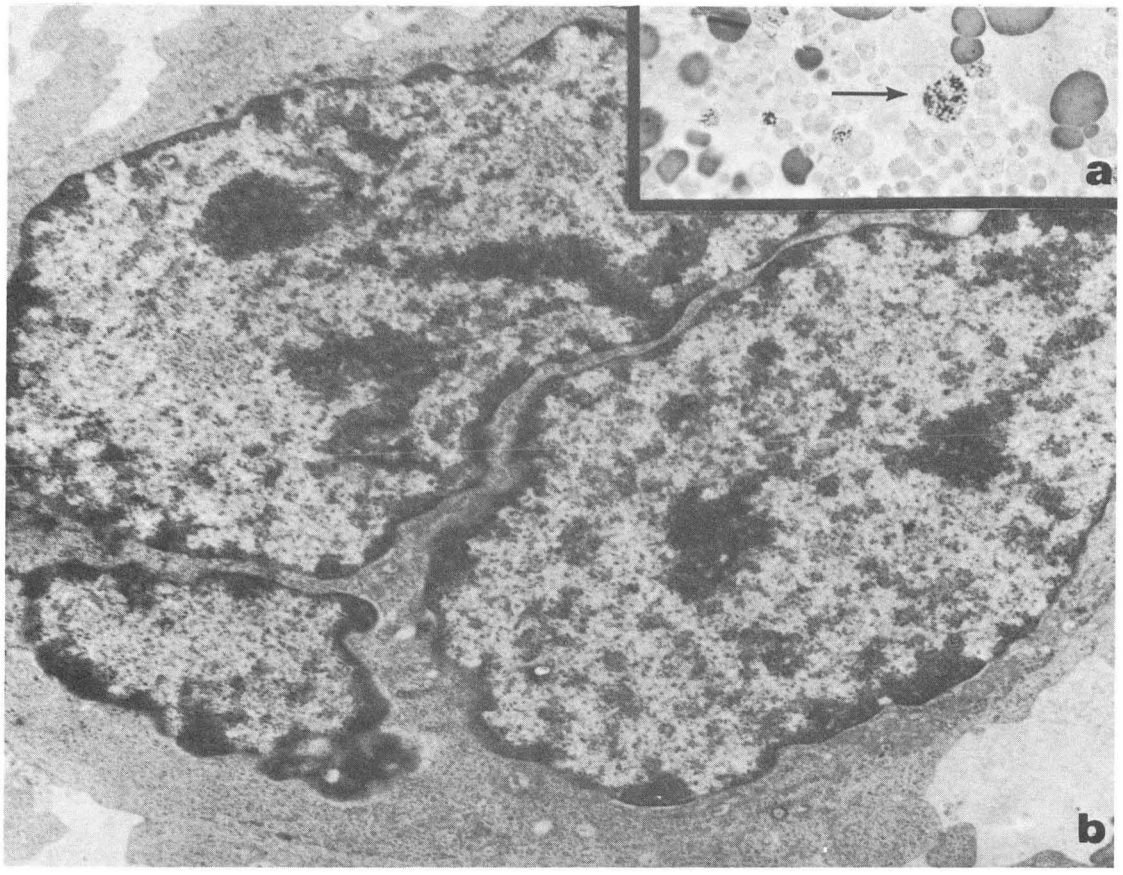

XBB 695-3502

Fig 7. "Immature" megakaryocyte synthesizing DNA. Arrow indicates labeled cell in low magnification picture of thick section (7a; X 650). Corresponding thin section shows large nucleus divided by internal cytoplasmic extensions (7b; X 14,800). Glutaraldehyde osmium fixation.

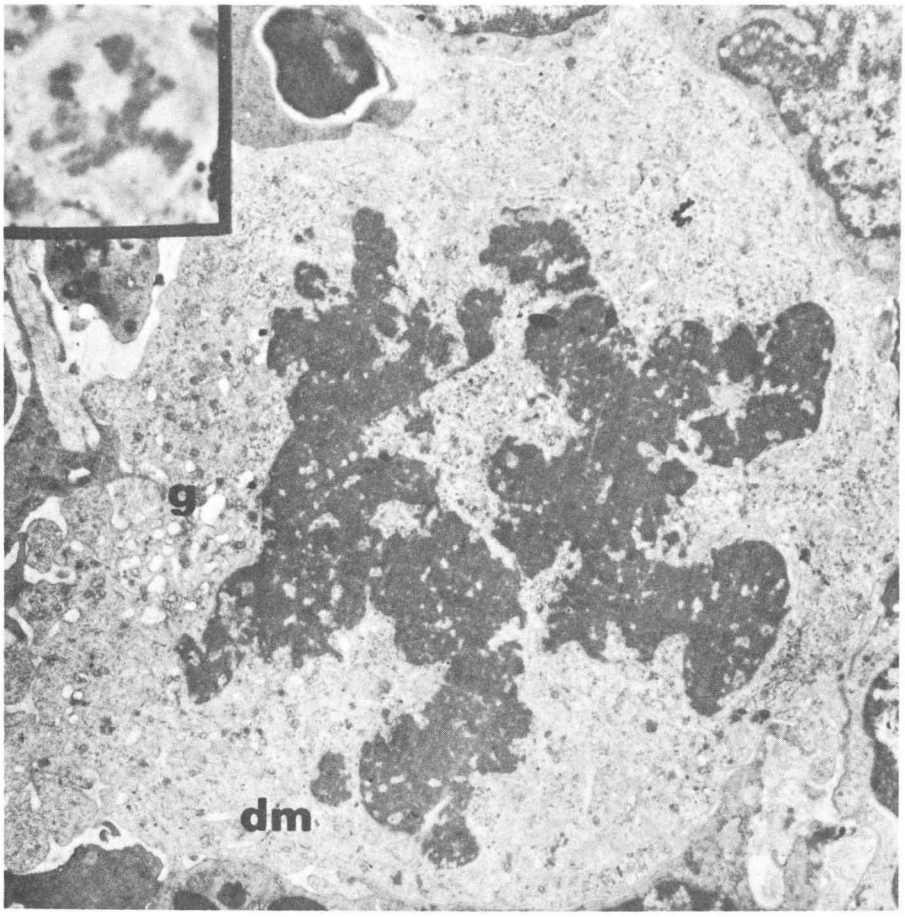

XBB 695-3214

Fig 8. "Immature" megakaryocyte in ana-telophase of mitosis showing Golgi apparatus, early granules and a few demarcation membranes. Mitosis, rather than nuclear degeneration, is proved by localized formation of nuclear membrane on condensed chromosomes and by absence of alterations in adjacent cells and in this cell's cytoplasm. Glutaraldehyde osmium fixation. Electron micrograph X 9000. Incerpt: phase contrast picture of adjacent thick section X 2100.

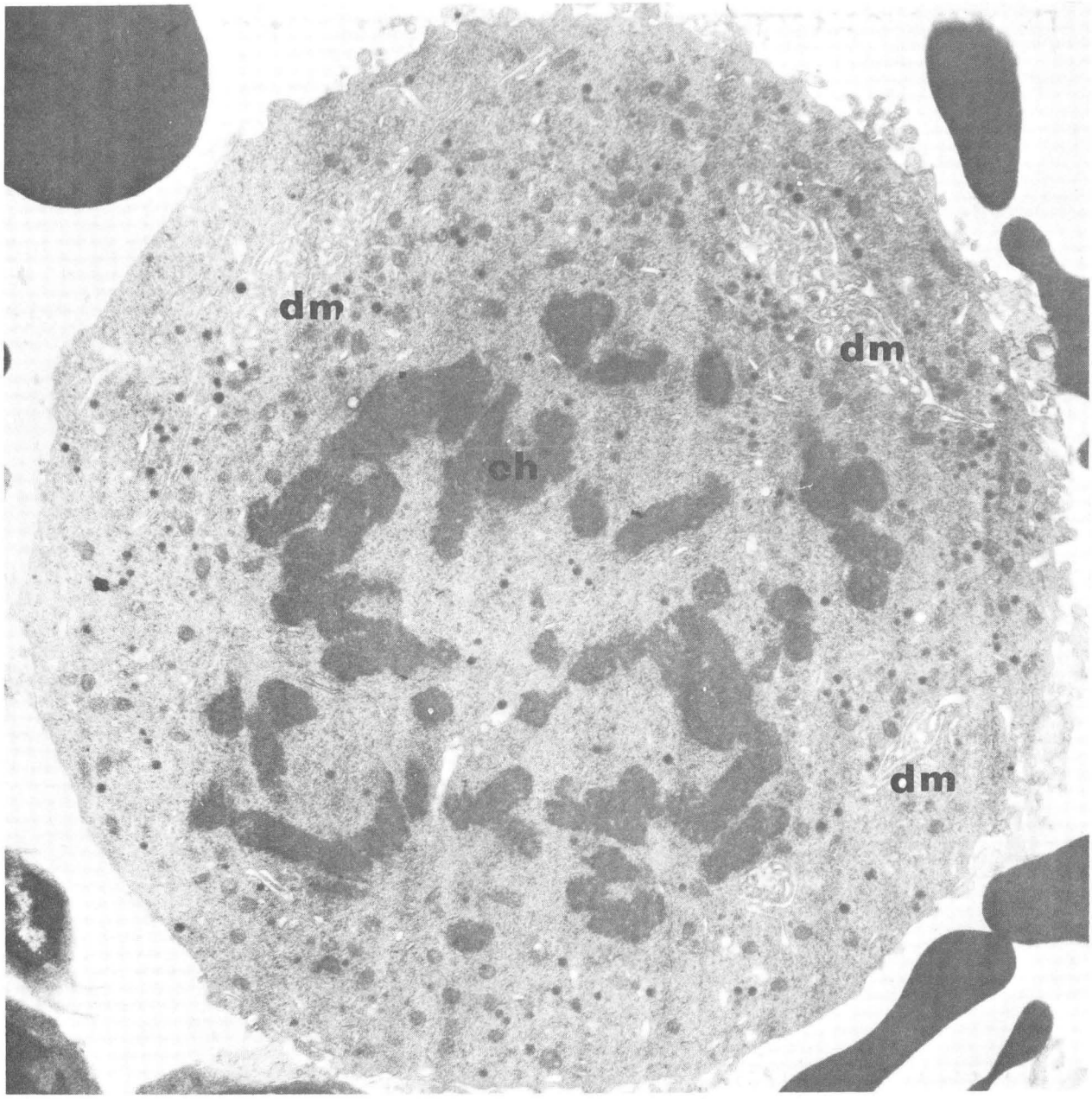

XBB 695-3504

Fig 9. "Immature" megakaryocyte in mitosis showing early formation of demarcation membranes. Rat marrow, glutaraldehyde osmium fixation X5700 (Courtesy Mrs. J. Breton-Gorius).

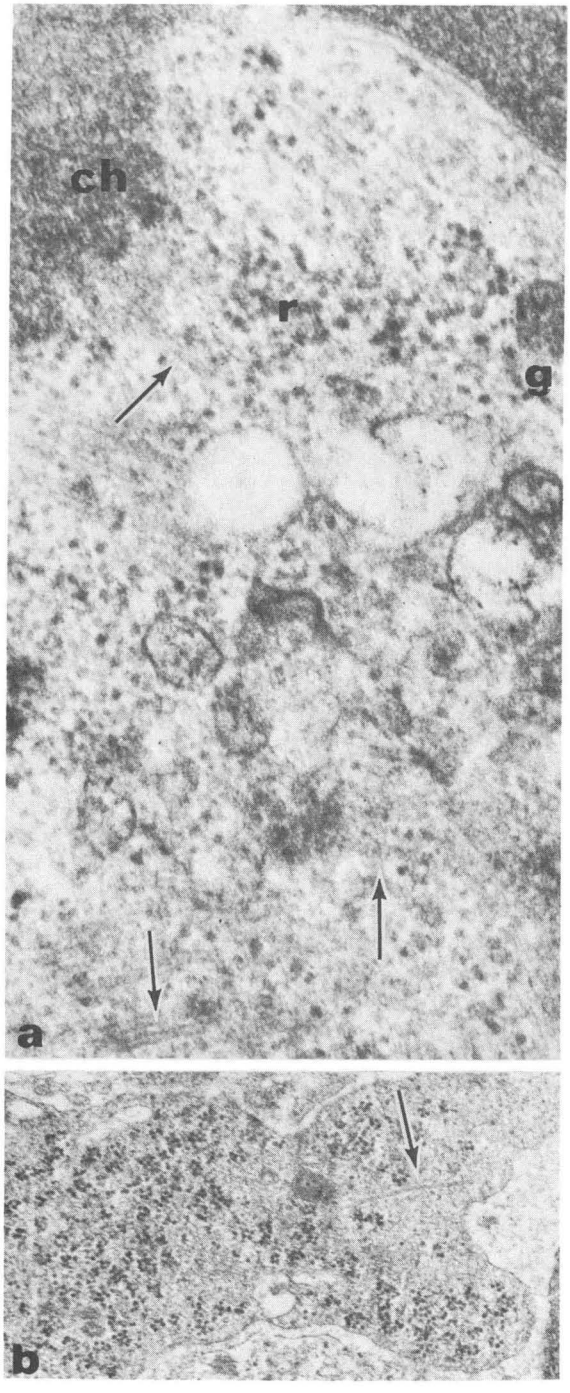

XBB 695-3505

Fig 10. Microtubules in immature megakaryocytes. 10a. Same cell as Fig 8. Some microtubules in Golgi zone point toward chromosome (top arrow). Nuclear membrane reappears at top right corner X 43,700. 10b. Microtubule seen in cytoplasmic extension of immature megakaryocyte. Glutaraldehyde osmium fixation X 34000.

immature aspect similar to that of younger cells (fig 13a). The outer zone contains myofibrils and microtubules. With progressive maturation, nucleoli and ribosomes present thus far, disappeared, while mitochondria became smaller and less numerous, and membrane formation and zonation became more conspicuous.

Thrombopoietic megakaryocytes were pycnotic cells, with a greatly enlarged and bubbling marginal zone (fig 14). Platelets were liberated through an opening of the vessel wall (figs 14 and 13d). In some cases the released platelets bore a hypertrophied peripheral zone contrasting with the near absence of this organelle in circulating platelets. The remaining of the megakaryocyte after thrombopoiesis consisted of a pycnotic nucleus with a narrow band of cytoplasm (fig 15). 15% of the megakaryocytes were found in this group.

Relationship Between Polyploidy and Cytoplasmic Maturation

The ploidy values reached peaks of frequency at 8N, 16N and 32N (fig 4). The proportion of these three classes was 20%, 67.5% and 12.5% respectively. No 4N megakaryocyte could be recognized. In the 32N and the 16N group, the coefficient of variation between individual megakaryocyte DNA content was 9 and 10% respectively (excluding immature cells).

Fig 16 shows a diagram of megakaryocyte maturation versus ploidy. For each cell the stage of cytoplasmic maturation and the degree of ploidy have been determined. Immature cells, able to synthesize DNA, were found at ploidy levels 8N to 22.1N (fig 11). Maturing and thrombopoietic megakaryocytes which had completed ploidization could be encountered at each of the three ploidy levels 8N, 16N or 32N. As an illustration of this observation, Fig 12 shows two megakaryocytes which have nearly identical submicroscopic appearance. One is a 16N, the other a 32N cell.

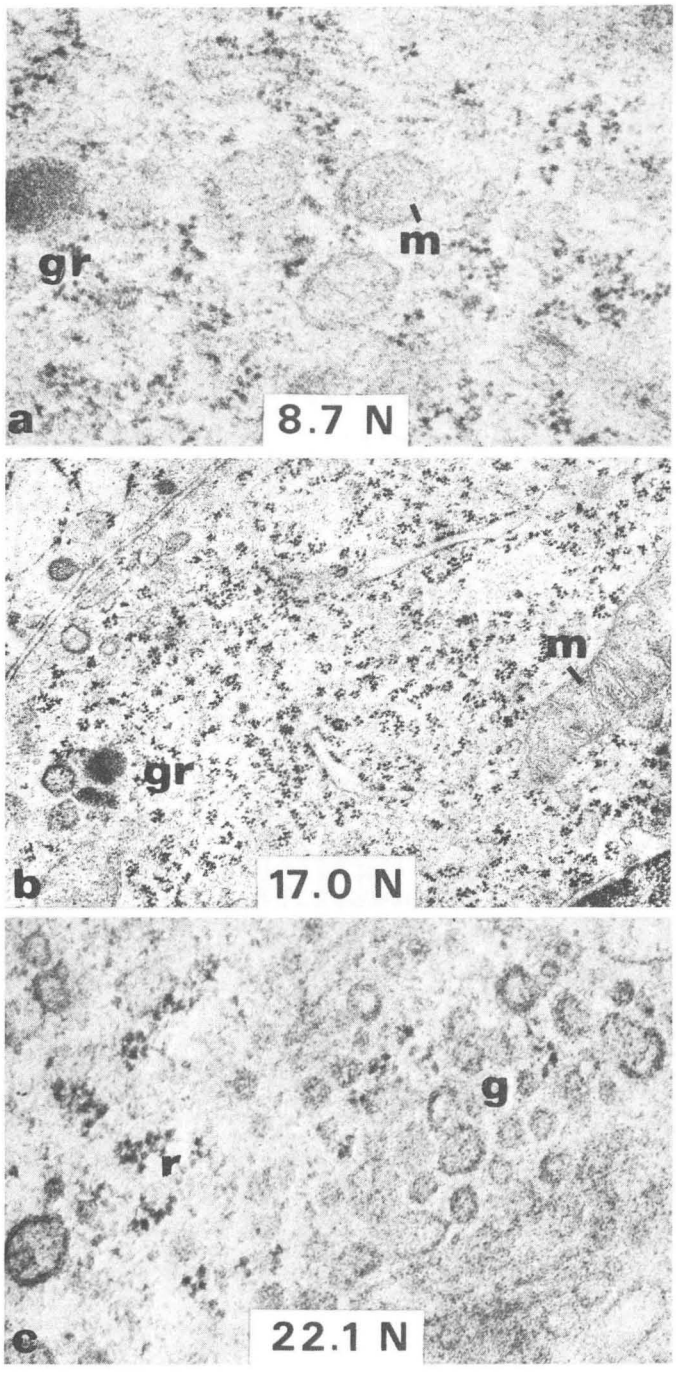

XBB 695-3503

Fig 11. "Immature" megakaryocytes at three different ploidy levels. a X 57300. b X 23600. c X 70000. Osmium fixation.

Study of thrombopoietic megakaryocytes was of particular interest since few analyses had been made on this stage before (17). Despite the fact that microphotometric error was relatively larger on the condensed, pycnotic nuclei of thrombopoietic cells, it was clear that thrombopoiesis could be observed at all three ploidy levels (figs 14, 15 and 16).

DISCUSSION

The Method

The technique of alternate thick and thin sectioning has been previously used to combine electron microscopy and autoradiography (30, 31). The present study shows that it also makes it possible to measure the relative amount of a cellular substance i.e. DNA in relation to the cell's ultrastructure, thus permitting the combination of quantitative cytochemistry and electron microscopy. The validity of this procedure is demonstrated by the following facts: 1) megakaryocyte nuclei of guinea pigs could be grouped in three ploidy classes namely 8N, 16N, and 32N (fig 4). 2) The proportion of these three classes was 20%, 67.5% and 12.5% respectively, to be compared with very similar values obtained by conventional microspectrophotometry in guinea pigs (12) and rats (13). 3) Among the 16N and 32N classes, the coefficient of variation of DNA content was 9 or 10%. This variation consists mainly of technical errors since biological dispersion around the class modal value is probably very small (32). Therefore, the precision of the method is sufficient to exclude an error of one ploidy class.

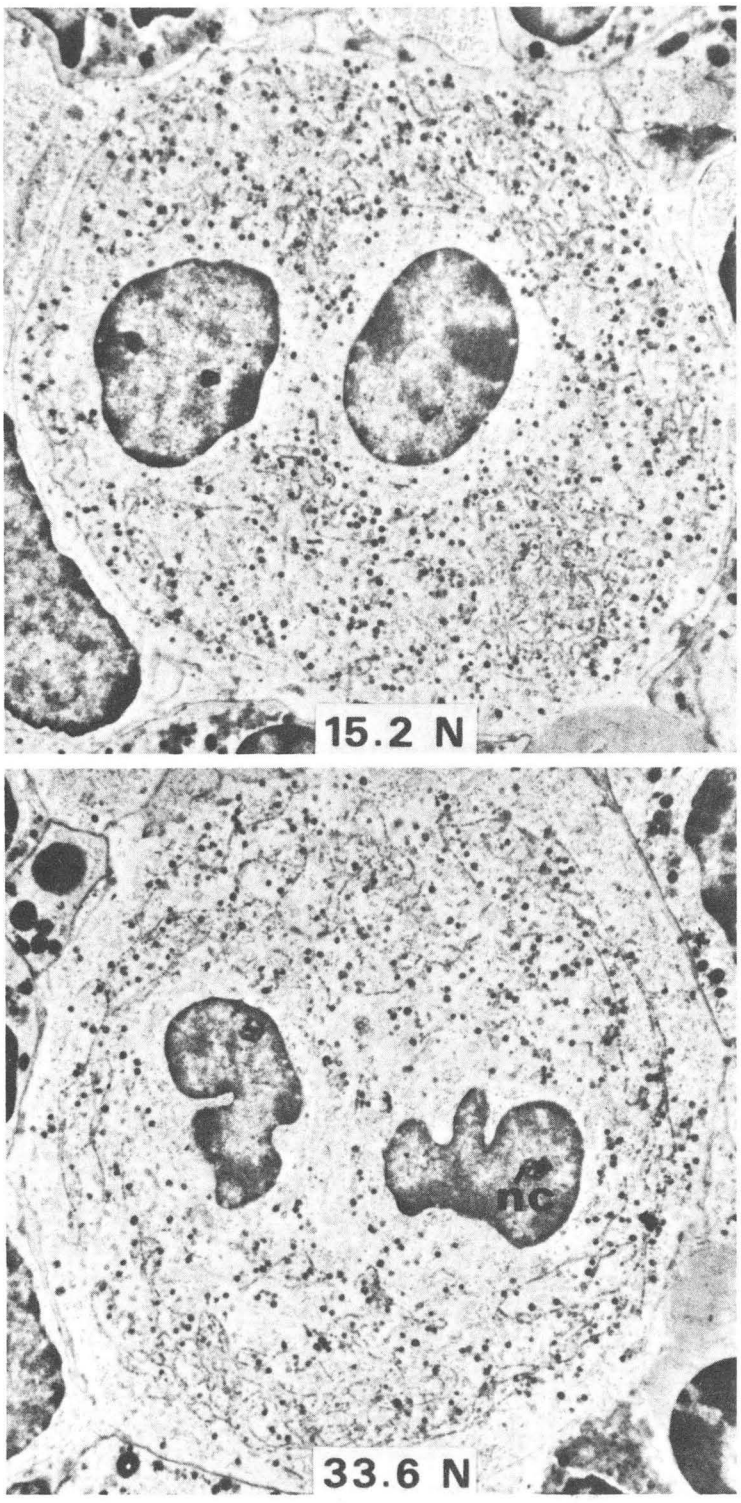

XBB 695-3213

Fig 12. Similar cytoplasmic organelle development in maturing megakaryocytes of different ploidy value. Osmium fixation X 6800.

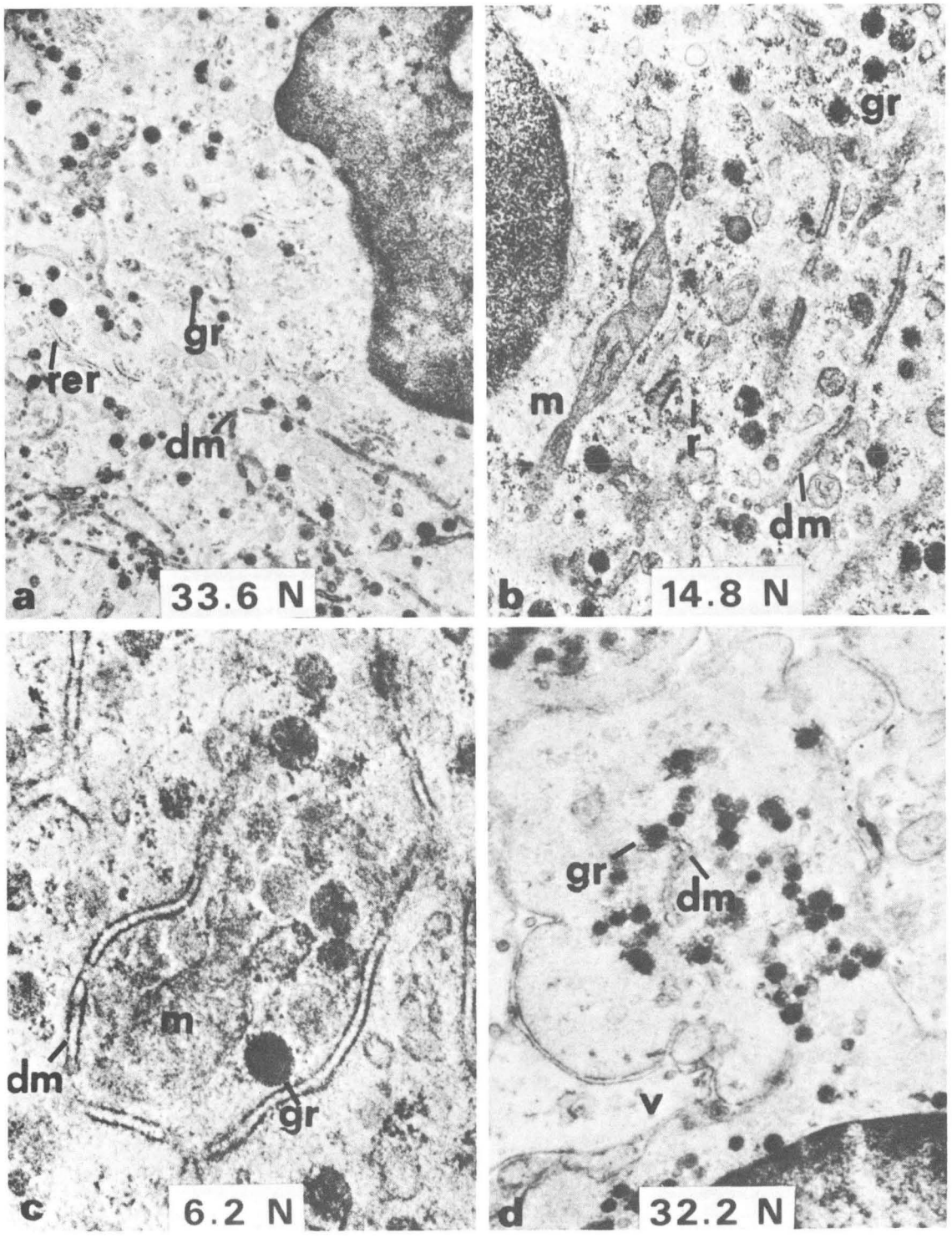

XBB 695-3212

Fig 13. Successive stages of cytoplasmic specialization in three maturing (a, b, c) and in one thrombopoietic (d) megakaryocyte. a, b, and c show development of demarcation membranes (dm) at different ploidy levels. d newly formed platelet protruding through vessel wall (v) (see Fig 14). Osmium fixation: a X 14,800. b X 26,000. c X 53,800. d X 17,600.

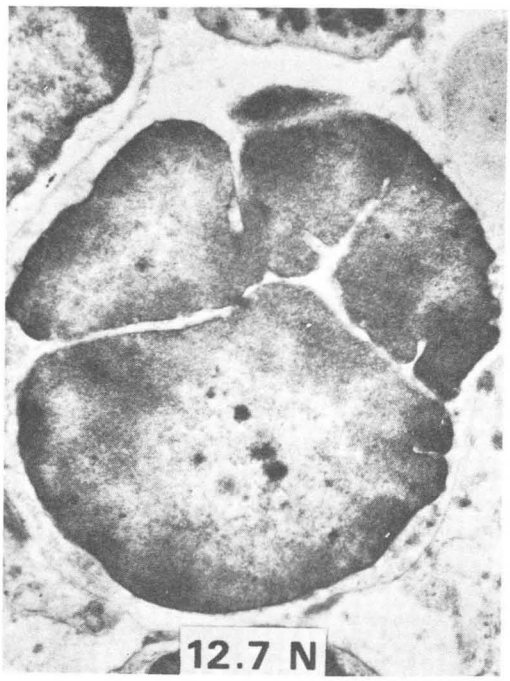

XBB 695-3216

Fig 14. Thrombopoietic megakaryocyte and five platelets (pl) liberated into vessel. Black squares indicate cell limits. Bubbling (bub) of hypertrophied peripheral zone. See Fig 13d. Osmium fixation X 3700.

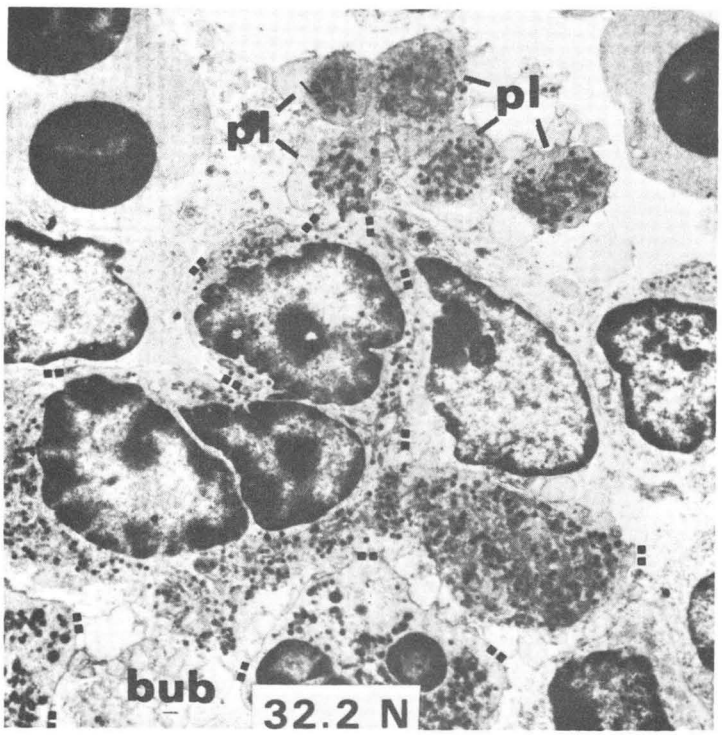

XBB 695-3217

Fig 15. Pycnotic megakaryocyte nucleus. Osmium fixation X 12600.

Pattern of Megakaryocyte Maturation

The present study proposes a middle way between two opposite conceptions of megakaryocyte maturation and shows that ploidization and development of cytoplasmic organelles are neither strictly parallel nor consecutive processes. Contrary to light microscopy autoradiography studies, and in partial agreement with the studies of Kinosita (33), ultrastructural analyses detect some early formation of specific organelles in immature megakaryocytes (figs 5 - 10). The reasons for this discrepancy are to be found not only in the superior resolving power of the electron microscope, but also in the particular localization of the early granules. While imprints fail to show the presence of the cytoplasmic endonuclear zone, sections demonstrate that the nucleus has in fact a hollow center which contains most of the Golgi apparatus and the early granules. The endonuclear cytoplasmic zone communicates with the outer cytoplasm (figs 5 and 6). Granule formation is not the only detectable sign of cytoplasmic maturation in immature cells; demarcation membranes, microtubules and microfibrils also appear during the ploidization phase. In addition, Odell et al. have shown that all recognizable cells of the thrombocytic series incorporate S^{35} into chondroitin sulfate (34, 35), the acid mucopoly saccharide presumably responsible for the alcian blue staining of demarcation membranes (35, 27).

The length of the ploidization phase can be inferred from ploidy measurements on cells such as maturing and thrombopoietic megakaryocytes which never synthesize DNA. These cells were found mostly in the 16N group and much less frequently in the 8N and 32N groups (fig 16; ref 17). Similar findings were made in light microscopy by de Leval (9) and Odell and Jackson (10). Thus, the common conclusion of light and electron microscopy studies is that the ploidi-

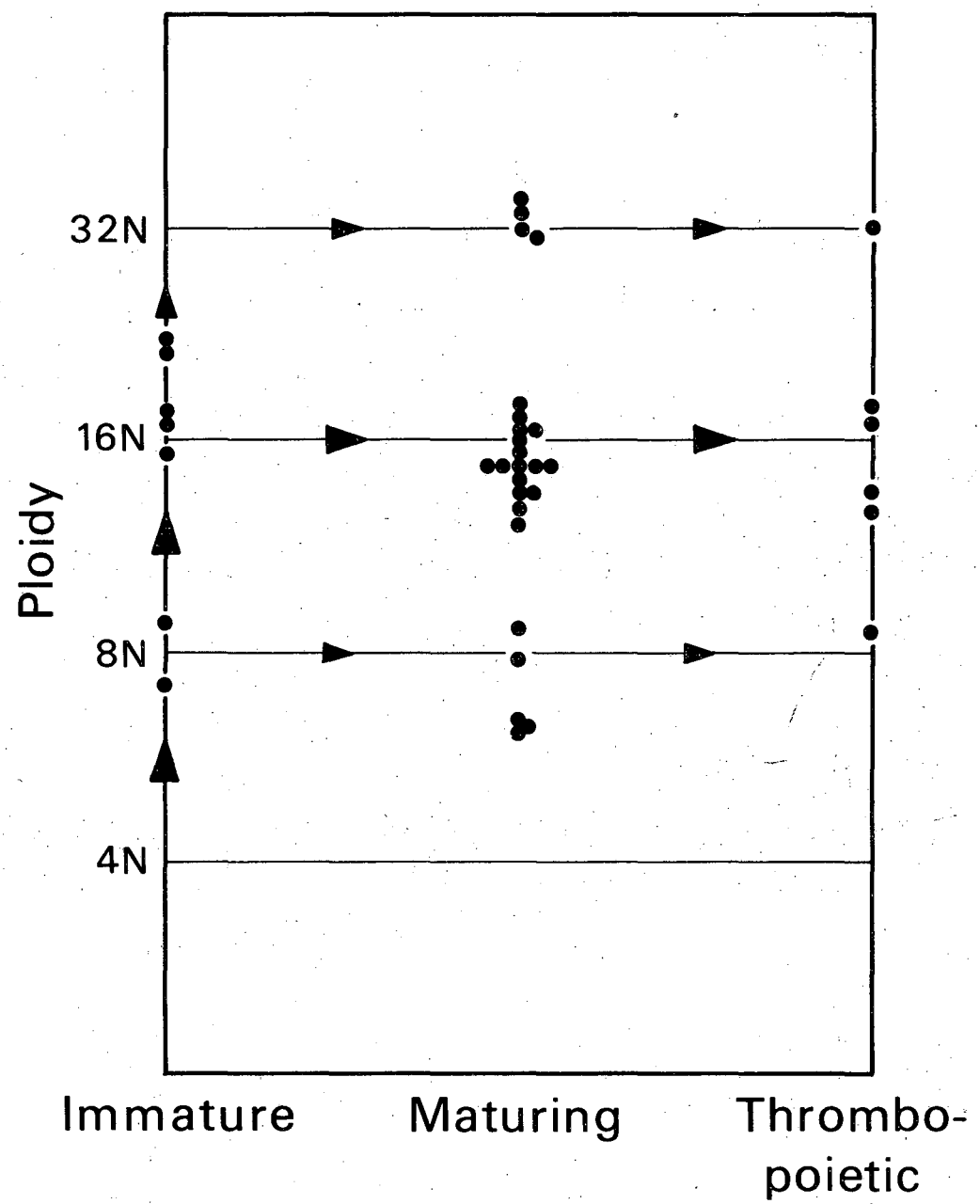

Fig 16. Diagram of ploidy values in developing megakaryocytes. Each point represents one cell.

zation phase comprises, on the average, 3 $\pm$ 0.5 (1 S.D.) genome duplications. This finding suggests a possible mechanism for the regulation of platelet production (37).

The end of ploidization is marked by several cytological changes. The nucleus is transformed into an irregularly segmented mass, a modification best observed in imprints (15), but evident in sections also. The Golgi apparatus tends to become totally exonuclear. The nuclear size remains constant (15) as cytoplasmic volume increases, thereby decreasing the nuclear-cytoplasmic ratio. Finally a massive synthesis of demarcation membranes and granules occurs and the latter become visible in light microscopy (9, 10). At this stage, it is possible to demonstrate platelet antigens (15) among which is thrombosthenin, present in granules and membranes (36).

It is thus apparent that organelle formation is initiated in immature megakaryocytes and reaches a peak after the ploidization phase. This pattern of megakaryocyte maturation bears some resemblance to specialization of the other marrow series. Granulocytes as well as megakaryocytes begin synthesizing granules in the Golgi apparatus during the phase of genome multiplication. In both series, nuclear segmentation accompanies the end of this phase. In addition, both erythrocytic and megakaryocytic series, after nuclear pycnosis, produce an enucleate element, the metabolic activities of which have many similarities (37).

SUMMARY

The thick and thin section technique was used to study guinea-pig megakaryocytes by electron microscopy combined with either autoradiography or cytophotometric determination of DNA. Granule formation began in the hollow center of the nucleus of megakaryocytes engaged in polyploidization. The ploidization phase stopped at the 8N, 16N or 32N level, after an average of 3 ± 0.5 (1 S.D.) genome duplications. Microtubules, myofibrilles and demarcation membranes were also present in the immature megakaryocytes but organelles were formed in increasing amounts in non DNA synthesizing cells. Platelet liberation, possible at the 8N, 16N or 32N stage, occurred in non DNA synthesizing cells, principally at the 16N level.

ACKNOWLEDGMENTS

This work has been possible thanks to the generous help and invaluable advice of Dr. M. Bessis, to whom we extend heartfelt thanks. We are also very grateful to Mrs. J. Breton-Gorius whose experience was indispensable in this study, and to Drs. G. Brecher, H. C. Mel and B. Thorell for their excellent criticism. We wish finally to acknowledge the skillful assistance of O. Pierre, Mrs. Maigne, M. Coumont, R. de Postel, and G. Zarka.

REFERENCES

1. Stockdale F.E., and Holtzer H.: DNA synthesis and myogenesis. Exptl. Cell Res. 24:508, 1961.

2. Makela O., and Nossal G.J.V.: Autoradiographic studies on the immune response. II. DNA synthesis amongst single antibody-producing cells. J. Exptl. Med. 115:231, 1962.

3. Gallien-Lartigue O. and Goldwasser E. On the mechanism of erythropoietin induced differentiation I. The effects of specific inhibitors of hemoglobin synthesis. Biochem. Biophys. Acta 103:319, 1965- Krantz S.B., and Goldwasser E. II. The effect on RNA synthesis. Biochem. Acta 103:325, 1965.

4. Stockdale F.E., and Topper Y.J.: The role of DNA synthesis and mitosis in hormone dependent differentiation. Proc. Nat. Acad. Sci.: 56:1283, 1967.

5. Ingram V.M.: Tadpoles, chicks and red cells: a study of development. Am. J. Human Genetics. 20:289, 1968.

6. Wessels N.K. and Rutter W.J.: Phases in cell differentiation. Sc. Amer. 220: 3, 36, 1969.

7. Feinendegen L.E., Odartchenko N., Cottier N., and Bond V.P. Kinetics of megakaryocyte proliferation. Proc. Soc. Exp. Biol. Med. 111:177, 1962.

8. Ebbe S., and Stohlman F. Jr.: Megakaryocytopoiesis in the rat. Blood 26:20, 1965.

9. de Leval, M.: Etude cytophotométrique et histoautoradiographique des acides désoxyribonucléiques au cours de la maturation mégacaryocytaire dans la moelle osseuse de cobaye (Cytophotometric and histoautoradiographic study of DNA during megakaryocyte maturation in guinea-pig bone marrow). C.R. Soc. Biol. 160: 2487, 1966.

10. Odell T.T. Jr., and Jackson C.W.: Polyploidy and maturation of rat megakaryocytes. Blood 32:102, 1968.

11. Garcia A.M.: Feulgen DNA values in megakaryocytes. J. Cell Biol. 20: 342, 1964.

12. de Leval M.: Dosages cytophotométriques d'ADN dans les mégacaryocytes normaux de cobaye (Cytophotometric measurements of DNA in normal guinea-pig megakaryocytes). C.R. Soc. Biol. 158:2198, 1964.

13. Odell T.T. Jr., Jackson C.W. and Gosslee D.G.: Maturation of rat megakaryocytes studied by microspectrophotometric measurement of DNA. Proc. Soc. Exp. Biol. Med. 119:1194, 1965.

14. de Leval M.: Etude cytochimique quantitative des acides désoxyribonucléiques au cours de la maturation mégacaryocytaire (Quantitative cytochemical study of DNA during megakaryocyte maturation). Nv.Rev. Franç. Hemat. 8:392, 1968.

15. de Leval M.: Contribution à l'étude de la maturation des mégacaryocytes dans la moelle osseuse de cobaye (Contribution to the study of megakaryocyte maturation in guinea-pig bone marrow). Arch. Biol. 79:597, 1968.

16. Paulus J.M.: Etude ultrastructurale et microphotométrique de la maturation mégacaryocytaire (Ultrastructural and microphotometric study of megakaryocyte maturation). Nv. Rev. Franc. Hemat. 8:394:1968.

17. Paulus J.M.: Cytophotometric measurements of DNA in thrombopoietic megakaryocytes. Exptl. Cell Res. 53:310, 1968.

18. Pease D.C.: Histological Techniques for Electron Microscopy. Academic Press, New York, 1964.

19. Deitch A.: Cytophotometry of nucleic acids. In: Wied G.L. (Ed.): Introduction to Quantitative Cytochemistry. Academic Press, New York, 1966 p. 327.

20. Leuchtenberger C., Doolin P.F. and Kutsakis A.H.: Buffered osmium tetroxide (OsO4) fixation for cytological and Feulgen microspectrophotometric studies of human rectal polyps. J. Biochem. Biophys. Cytol. 1:385, 1955.

21. Sundelin P., Wartiovaara J., Saxen L. and Thorell B.: Increased cytoplasmic RNA reflecting an early step of inductive tissue interaction. Exptl. Cell Res. 54:347, 1969; and Thorell B.: personal communication.

22. Sondhaus C.A. and Thorell B.: Microspectrophotometric determination of non-heme iron in maturing erythroblasts and its relationship to the endocellular hemoglobin formation. Blood 16:1285, 1960.

23. Grasso J.A., Woodward J.W. and Swift H.: Cytochemical studies on nucleic acids and proteins in erythrocytic development. Proc. Nat Acad. Sci. 50:134 1963.

24. Rubini J.R., Keller S. and Cronkite E.P.: In vitro labeling of bone marrow and leukemic blood leucocytes with tritiated thymidine I. Physical and chemical factors which affect autoradiographic labeling. J. Lab. Clin. Med. 66:483, 1965.

25. Reynolds E.S.: The use of lead citrate at high pH as an electron-opaque stain in electron microscopy. J. Cell Biol 17:208, 1963.

26. Bessis M.: Cytology of the Blood and Blood Forming Organs. Grune and Stratton, New York, 1956.

27. Behnke O.: An electron microscope study of the megakaryocyte of the rat bone marrow. I. The development of the demarcation membrane system and the platelet surface coat. J. Ultrastructure Res. 24:412, 1968.

28. Jones O.P.: Normal granulopoiesis of the megakaryocyte. Proc. Eighth Congr. Europ. Soc. Hemat. New York, Karger, 1961 p. 429.

29. Yamada E.: The fine structure of the megakaryocyte in the mouse spleen. Acta Anat. 29:267, 1957.

30. Zajdela F. and Moreno G. Aspect au microscope électronique des cellules du sang circulant incorporant la thymidine (Electron microscopic aspect of circulating cells of the blood incorporating thymidine). Nv. Rev. Franc Hemat 3:65, 1963.

31. Orlic D. Gordon A.S. and Rhodin J.A.G.: Ultrastructural and autoradiographic studies of erythropoietin-induced red cell production. Ann. N.Y. Acad. Sci. 149:198, 1968.

32. Alpen E. and Johnston M.E.: Deoxyribonucleic acid content of mitotic nuclei of two mouse tumours. Nature 211:715, 1966.

33. Kinosita R., and Ohno S.: Biodynamics of thrombopoiesis. In: Blood Platelets, Henry Ford Hosp. Symp. Boston, Little Brown and Co. 1961 p. 611.

34. Odell T.T. Jr. and McDonald T.P.: Two mechanisms of sulfate S^{35} uptake by blood platelets of rats. Am. J. Physiol. 206:580, 1964.

35. Anderson B. and Odell T.T.: Chemical studies of mucopolysaccharides of rat blood platelets. Proc. Soc. Exp. Biol. Med. 99:765, 1958.

36. Nachman R.L. Marcus A.J. and Safier L.B.: Platelet thrombosthenin: subcellular localization and function. J. Clin. Investig. 46:1380, 1967.

37. Paulus J.M.: Multiple differentiation in megakaryocytes and platelets. Blood 29:407, 1967.

TECHNICAL INFORMATION DIVISION
LAWRENCE RADIATION LABORATORY
UNIVERSITY OF CALIFORNIA
BERKELEY, CALIFORNIA 94720